Proceedings of the 13th
IEEE International Conference on Nanotechnology
Beijing, China, August 5-8, 2013

Nanodiamond as a multimodal platform for drug delivery and radiosensitization of tumor cells

T. Petit[1], H.A. Girard[1], M. Combis-Schlumberger[1], R. Grall[2], J. Delic[2], S. Morel-Altmeyer[2], P. Bergonzo[1], S. Chevillard[2] and J.C. Arnault[1]

[1]CEA, LIST, Diamond Sensors Laboratory, F-91191 Gif-sur-Yvette, France
[2] CEA, Institute of Cellular and Molecular Radiobiology, Laboratory of Experimental Cancerology, F-92265 Fontenay-aux-Roses, France

Email: jean-charles.arnault@cea.fr, hugues.girard@cea.fr

***Abstract* — Nanodiamonds (NDs) are often considered as inert platforms with high interests for biomedical applications. They are well adapted for drug delivery, and may display embedded fluorescence. We report here on a new way to consider these nanocarbon particles, by revealing therapeutic capacities coming from electronic properties of NDs. With an optimized surface chemistry, the generation of Reactive Oxygen Species (ROS) occurs when those hydrogen-terminated NDs are exposed to photon irradiation, thus opening up the field towards the radiosensitization of tumor cells.**

Index Terms – Nanodiamonds, hydrogen, zeta potential, radiosensitization, drug delivery

I. Introduction

Nanodiamonds are constituted of a diamond core surrounded with amorphous carbon and surface terminations, i.e. chemical functions which saturate the dangling bonds of the diamond lattice. In that sense, they reproduce at the nanoscale the typical bulk diamond structure. Then, applications of NDs usually focus on these diamond bulk properties translated at the nanoscale. For example, the hardness of NDs is used to increase the stability of supercapacitors [1] or the mechanical properties of new composite materials [2]. Toward more biological uses, NDs benefit from the biocompatibility of the bulk material and its intrinsic luminescent properties, arising from highly stable nitrogen vacancy (NV) colored centers [3–5]. They also take advantage of their diamond surface chemistry, based on covalent carbon-carbon chemistry, highly convenient for functionalization. These bulk properties combined to their high surface-to-volume ratio make them of great interest for nanomedical applications. For instance, starting from efficient plasma, chemical or thermal treatments to homogenize their surface chemistry [6], NDs have been successfully conjugated with oligonucleotides [4], [5], antibodies [7] or anti-cancer drugs [8]. Here, the diamond core is considered as an inert platform, often housing luminescence properties for diagnostic.

However, unexpected surface properties related to nanoscaled effects may occur on the smallest NDs. In particular, NDs synthesized by detonation method, exhibiting a size of approximately 5 nm, have shown astonishing properties such as an exceptional colloidal stability [9], [10], a giant permittivity [11] or unusual charge exchange properties [12] which are hardly explained by the assets of their diamond core only. Furthermore, these phenomena are thought to result from interactions with surrounding molecules, enhanced by their high surface-to-volume ratio, and thus may depend strongly on the NDs surface chemistry. Among typical surface terminations of diamond, hydrogen is known to confer specific properties to the material. In particular, hydrogen-terminated bulk diamond exhibits a negative electron affinity (NEA), at the origin of a p-type surface conductive layer after air exposure [13], [14] leading to a unique chemical reactivity [15], [16]. In water, an electrochemical exchange with a redox couple involving oxygen occurs even with intrinsic diamond [17].
In this study, we propose to investigate in which extent such hydrogenated terminations can affect the colloidal and electronic properties of 5 nm NDs toward drug delivery and radiosensitization applications.

II. Experimental

Materials: Detonation nanodiamonds (NDs) were provided by the Nanocarbon Research Institute. Hydrochloric acid, sulfuric acid and sodium hydroxide (Sigma-Aldrich) were used as received.
Plasma hydrogenation of nanodiamonds: 80-100 mg of NDs were deposited in a quartz tube and inserted in a plasma Downstream source (Sairem) (Figure 1). High purity hydrogen gas (>N70) was injected in the tube at a pressure of 15 mbar and plasma was generated in the quartz tube with a microwave power of 300 W (2.45 GHz). During the plasma, the tube was air cooled. NDs were exposed to hydrogen plasma for 15 minutes and were cooled down under hydrogen, leading to H-NDs.

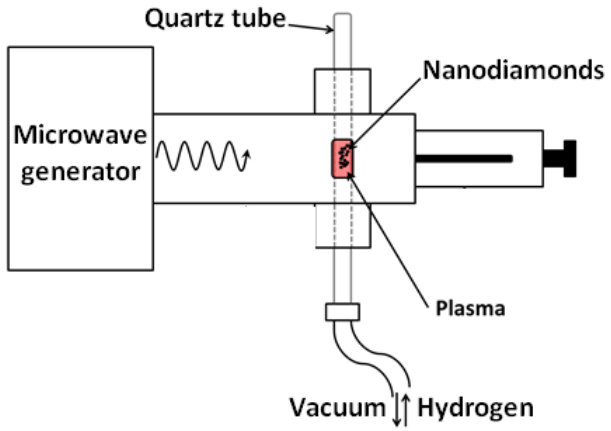

Figure 1. Experimental set-up for nanodiamond hydrogenation

Preparation of nanodiamond dispersions: NDs-H were dispersed in ultrapure water by sonication (Hielscher UP400S, 300W, 24 kHz) for 2h under cooling. Larger aggregates were removed from the solution by 1h centrifugation at 4000 rpm. Oxidized NDs are obtained by air annealing (400°C for 2 hours) and dispersed in ultrapure water by a similar method.

Zeta Potential/Titration: Size and Zeta potential (ZP) measurements of NDs-H suspensions were performed in ultrapure water on a Nanosizer ZS (Malvern) in the back scattering configuration (173°). pH-titration of the ZP was monitored using a Malvern autotitrator module (MPT-2) with HCl 0.1 M and NaOH 0.1 M as acidic and basic titrants. Acid titrations where also performed using the same autotitrator module with HCl 0.1 M and H2SO4 0.05 M under mild magnetic steering. For each pH value or acid concentration, three independent ZP and size measurements were made after recirculating the solution.

Cell cultures : Caki-1 cells (ATCC number: HTB-46) were grown at 37°C in a humidified atmosphere of 5% CO2 and 9 % air, in Dulbecco's modified Eagle medium (DMEM) glutamax supplemented with 10% (v/v) heat inactivated fetal bovine serum and 1 mM antibiotic-antimycotic (penicilline-streptomycine; Invitrogen).

Cytotoxicity real-time follow-up (XCelligence, Roche Diagnostics) and treatments : Cells were seeded on 96 wells-microplate (5x103 cells/well) in contact with electrodes for continuous measuring cell impedance (E plates, Roche Diagnostics)), incubated for 30 min at 37°C and placed in the Real-Time Cell Analyzer (RTCA) station (Roche Diagnostics). Cells were grown for 24 h before H-NDs exposure to at concentrations of 10, 100, and 500 µg/ml. Cells were exposed to gamma-rays at 4 Gy, 1Gy/min using a cesium irradiator (IBL637 CisBio irradiator), 15 minutes after H-NDs addition,. Cytotoxicity of H-NDs and of radiation was monitored by measuring cell impedance every 5 min for 6 h and then every 10 min for 24 h. Cell index (CI) was calculated as follows: Zi-Z0 [Ohm]/15[Ohm]; where Z0: is the background impedance and Zi: the individual time point impedance. Cell index was normalized as function of the CI value measured just before the exposure with nanoparticles.

Reactive oxygen species (ROS) quantification by flow cytometry : One hour and 24 h after treatment, either H-NDs, irradiated, or both, cells were washed twice in PBS, trypsinized, centrifuged for 5 min at 300xg and then re-suspended in 5 mL of complete medium. For ROS analysis, $5x10^5$ cells per condition were incubated with H2DCFDA probe (final concentration of 2µM) (Molecular Probes, Invitrogen) at 37°C for 10 min,centrifuged for 5min at 300xg, re-suspended in 500µL of PBS containing 5% serum, incubated at 37°C for 20 min and washed again in PBS just before flow cytometry analysis (BD Facscalibur and FlowJo 7.5.5 software). Multi-parametric analyses were performed: a first analysis was done according to cell size/granulometry, discriminate living and dead cells while removing fragmented cells. This first step allowed us to gate at least $2x10^4$ cells per replica. Then, once tuned on this setting, the ROS/H2DCFDA signal was collected on FL1 (λ em: 517/27 nm) after laser excitation at 488 nm (H-NDs do not interfere with this dye). The results were reported as the mean distribution of cell fluorescence (3 replicas ,(with at least $2x10^4$ gated cells per replica).

III. Results & Discussions

Hydrogenated NDs (H-NDs) are obtained from oxidized NDs by microwave-enhanced plasma treatment [18-20]. Such plasma treatments efficiently passivate the ND surfaces with hydrogen atoms while etching non-diamond carbon and oxygen species. From a raw hydrogenated powder, a suspension of H-NDs can be prepared. Dynamic light scattering (DLS) measurements were performed (Malvern Nanosizer ZS) to investigate the size distribution and the zeta potential of H-NDs, as shown in Fig. 2. DLS characterizations of oxidized NDs are also reported for comparison. On oxidized NDs, a mean diameter of 10 nm is measured, which is close to the primary size of the particles (5 nm). They exhibit a negative zeta potential below -30 mV from pH=4 to at least pH=10, linked to their carboxylated surface. After hydrogenation, NDs are slightly more aggregated, with a mean diameter close to 30 nm. In the same time, their zeta potential switches to positive values, reaching over +30 mV from pH=4 to pH=10. This positive zeta potential directly originates from surface electronic properties of hydrogenated diamond. As for hydrogenated bulk diamond, an electrochemical equilibrium with adsorbed oxygen species is created on H-NDs surface when exposed to air or water. As a consequence, a surface band bending occurs at the H-NDs surface, generating a hole accumulation, similar to a p-doped layer. This phenomenon, well known on hydrogenated bulk diamond, leads on H-NDs to a high positive zeta potential between pH=4 to pH=10, as shown on Fig. 2. Above pH=10, the electrochemical equilibrium is modified, resulting in a weaker band bending and consequently a lower zeta potential, as described by Chakrapani and coworkers [17]. In this model, a high concentration of adsorbed oxygen on H-NDs is required to generate the equilibrium. X-ray Photoemission Spectroscopy (XPS) analysis performed on H-NDs after dispersion in

water confirmed the presence and of this oxygen species on their surface and their role on their surface electronic properties [21]. Furthermore, it has been shown that this oxygen can be removed by flushing the suspension of H-NDs with N_2, which results in the flocculation of the particles.

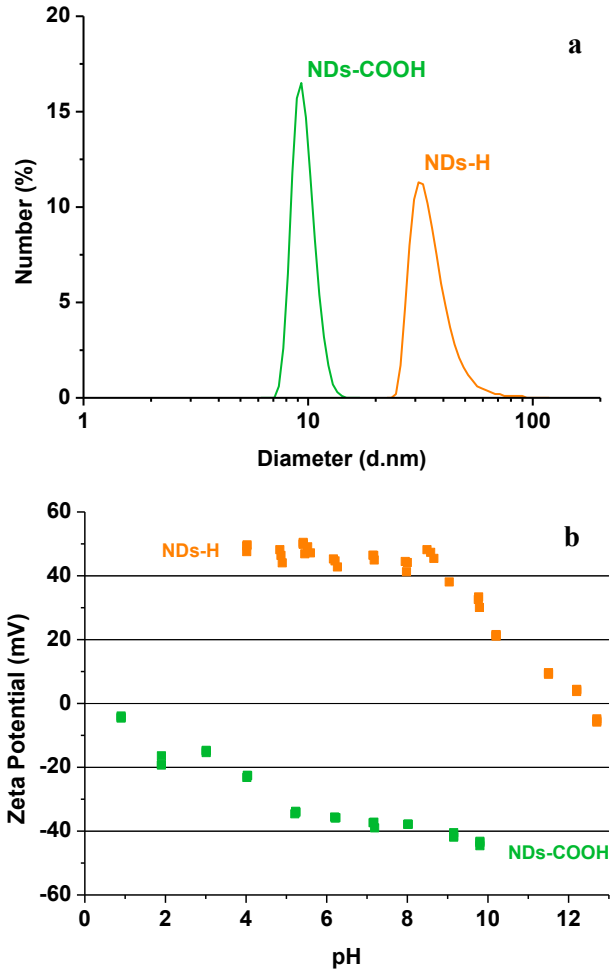

Figure 2. (a) Size distribution and (b) Zeta potential evolution versus pH for NDs-H and NDs-COOH in water.

A high positive zeta potential is provided by hydrogenation to the particles, which is highly desirable, notably for gene delivery. If a negative charge can be easily conferred to NDs by a carboxylation, the generation of a positive zeta potential still constitutes an issue. Indeed, previous works reported on the use of cumbersome polymeric coating to obtain such positive charges on NDs [5], but accompanied with a raise of diameter and possible toxic drawbacks. Here, the diameter is preserved and the suspensions remain perfectly stable, rendering our H-NDs ideal candidates for drug delivery matters.

In addition to the transfer doping at the origin of their positive charge, hydrogenated NDs also exhibit a negative electron affinity. The presence of this NEA has already been demonstrated onto 50 nm H-NDs [20] and is in accordance with the transfer doping which occurs on our 5 nm NDs. The combination of this NEA and the high concentration of oxygen species adsorbed on H-NDs surface may be advantageous toward biomedical application. Under irradiation, this NEA can facilitate the emission of electrons at the surface of the particle, rich of oxygen species, thus generating an efficient source of reactive oxygen species (ROS) for radiosensitization.

Kidney human cancer cell line Caki-1 were thus exposed to different doses of H-NDs, ranging from 10 to 500 µg/mL, and irradiated or not with 4Gy gamma rays. Note that this cell line was chosen because it is representative of the kidney tumor radiosensitivty. The cytotoxicity was measured by impedancemetry since it permits a continuous real time analysis of cell response (CI) and it was shown that nanoparticles alone do not induce any artifactual variation of impedance [22]. Variation of cell impedance reflects changes in cell morphology, proliferation, adhesion and membrane potential. CI measured 96h are reported in Figure 3 for H-NDs treated cells with or without radiation exposure. First, without irradiation, one can notice the absence of cytotoxicity of H-NDs up to 100 µg/mL and the very low cytotoxicity at the high concentration of 500 µg/mL. After irradiation, a strong radiosensitizating effect is observed, even for the lowest dose of H-NDs of 10 µg/mL. It should be noticed that the effect is not a dose dependent radiosensitization, suggesting that the induced effect is already maximum at the lowest dose.

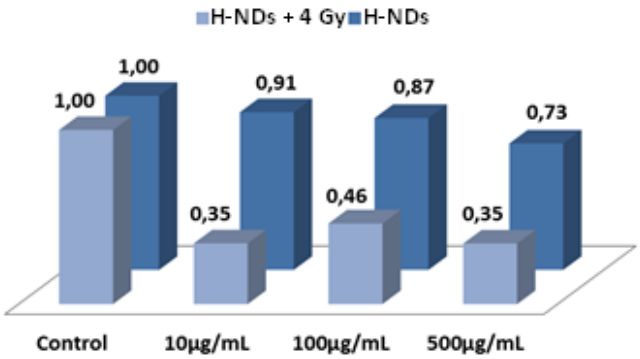

Figure 3. Evolution of the cellular indexes (impedance) at 96h of Caki-1 cells treated with H-NDs alone or combined with γ-irradiation (4 Gy).

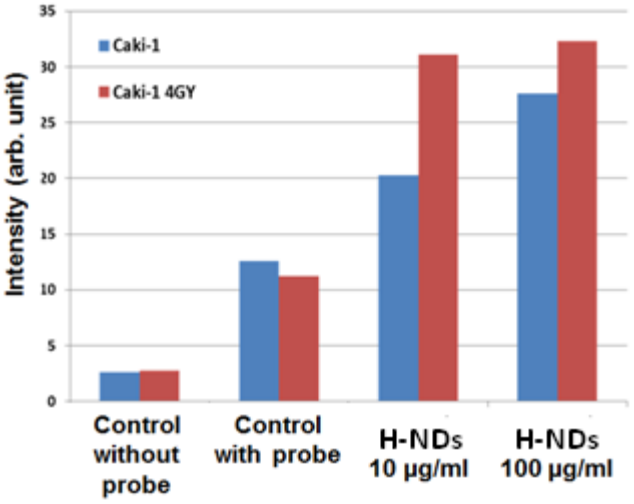

Figure 4. Intracellular ROS quantification in cell line Caki-1 following H-NDs single treatment or H-NDs combined with γ-irradiation (4Gy). Probe : (2',7'-dichlorofluorescein, DCF)

In order to determine the role of the oxidative stress in the radiosensitizing effect of H-NDs, we analysed by flow cytometry the level of intracellular ROS (H2DCFDA probe) after H-NDs or combined H-NDs-radiation exposure. As the measurements were performed one hour after radiation exposure, the level of ROS cannot be ascribed to the primary radiation oxidative stress effect, which occurs within seconds after radiation exposure, but rather to a secondary oxidative stress related to the irradiation of H-NDs. In H-NDs exposed cells, an increased level of ROS is observed compared to the control, that can be due to a high concentration of oxygen species surrounded NDs. However, taking into account the profiles of cytotoxicity for equivalent doses (Figure 3), these levels of ROS does not seem to induce significant cellular effects. On the opposite, when cells are exposed to both H-NDs and irradiation, a clear raise of the ROS generation is observed in the treated cells, in a concomitant way with the drop of the cellular indexes, suggesting that ROS effectively participate to the radiosensitizating effect. These original data suggest potential application of H-NDs in bio-medical domain that warrants further biological investigations.

IV. Conclusions

Carrying a positive zeta potential desirable for delivery, and offering a diamond core with therapeutic potentialities, H-NDs have now reached a maturity for nanomedicine. Instead of an efficient but inert platform, we demonstrated that NDs and more specifically H-NDs should now be considered as an active nanomaterial.

Acknowledgement

The authors would like to thank the financial support from the French Atomic Commission

References

[1] I. Kovalenko, D. G. Bucknall, and G. Yushin, "Detonation Nanodiamond and Onion-Like-Carbon-Embedded Polyaniline for Supercapacitors," *Advanced Functional Materials*, vol. 20, no. 22, pp. 3979–3986, Nov. 2010.

[2] V. Mochalin, I. Neitzel, and B. Etzold, "Covalent incorporation of aminated nanodiamond into an epoxy polymer network," ACS Nano, vol. 5, no. 9, pp. 7494–7502, Aug. 2011.

[3] Y.-R. Chang, H.-Y. Lee, K. Chen, C.-C. Chang, D.-S. Tsai, C.-C. Fu, T.-S. Lim, Y.-K. Tzeng, C.-Y. Fang, C.-C. Han, H.-C. Chang, and W. Fann, "Mass production and dynamic imaging of fluorescent nanodiamonds," *Nat Nano*, vol. 3, no. 5, pp. 284–288, 2008.

[4] X.-Q. Zhang, M. Chen, R. Lam, X. Xu, E. Osawa, and D. Ho, "Polymer-functionalized nanodiamond platforms as vehicles for gene delivery.," *ACS nano*, vol. 3, no. 9, pp. 2609–16, Sep. 2009.

[5] [1] A. Alhaddad, M. Adam, J. Botsoa, G. Dantelle, S. Perruchas, T. Gacoin, C. Mansuy, S. Lavielle, C. Malvy, and F. Treussart, "Nanodiamond as a vector for siRNA delivery to Ewing sarcoma cells," Small, vol. 7, no. 21, pp. 3087–3095, 2011.

[6] A. Krueger and D. Lang, "Functionality is Key: Recent Progress in the Surface Modification of Nanodiamond," *Advanced Functional Materials*, vol. 22, no. 5, pp. 890–906, 2012.

[7] A. H. Smith, E. M. Robinson, X.-Q. Zhang, E. K. Chow, Y. Lin, E. Osawa, J. Xi, and D. Ho, "Triggered release of therapeutic antibodies from nanodiamond complexes," *Nanoscale*, vol. 3, no. 7, pp. 2844–2848, 2011.

[8] E. K. Chow, X.-Q. Zhang, M. Chen, R. Lam, E. Robinson, H. Huang, D. Schaffer, E. Osawa, A. Goga, and D. Ho, "Nanodiamond Therapeutic Delivery Agents Mediate Enhanced Chemoresistant Tumor Treatment," *Science Translational Medicine*, vol. 3, no. 73, p. 73ra21, Mar. 2011.

[9] M. Ozawa, M. Inaguma, M. Takahashi, F. Kataoka, A. Krueger, and E. Osawa, "Preparation and behavior of brownish, clear nanodiamond colloids," *Advanced Materials*, vol. 19, no. 9, p. 1201, 2007.

[10] O. A. Williams, J. Hees, C. Dieker, W. Jäger, L. Kirste, and C. E. Nebel, "Size-Dependent Reactivity of Diamond Nanoparticles," *ACS Nano*, vol. 4, no. 8, pp. 4824–4830, 2010.

[11] [1] S. Batsanov and S. Gavrilkin, "Giant dielectric permittivity of detonation-produced nanodiamond is caused by water," Journal of Materials Chemistry, vol. 22, p. 11166, 2012.

[12] S. Stehlik, T. Petit, H. A. Girard, J.-C. Arnault, A. Kromka, and B. Rezek, "Nanoparticles Assume Electrical Potential According to Substrate, Size, and Surface Termination," *Langmuir*, vol. 29, no. 5, pp. 1634–1641, Jan. 2013.

[13] M. I. Landstrass and K. V Ravi, "Resistivity of chemical vapor deposited diamond films," *Applied Physics Letters*, vol. 55, no. 10, pp. 975–977, Sep. 1989.

[14] F. Maier, M. Riedel, B. Mantel, J. Ristein, and L. Ley, "Origin of Surface Conductivity in Diamond," *Physical Review Letters*, vol. 85, no. 16, pp. 3472–3475, Oct. 2000.

[15] W. S. Yang, O. Auciello, J. E. Butler, W. Cai, J. A. Carlisle, J. Gerbi, D. M. Gruen, T. Knickerbocker, T. L. Lasseter, J. N. Russell, L. M. Smith, and R. J. Hamers, "DNA-modified nanocrystalline diamond thin-films as

stable, biologically active substrates," *Nat. Mater.*, vol. 1, no. 4, pp. 253–257, 2002.

[16] A. Hartl, E. Schmich, J. A. Garrido, J. Hernando, S. C. R. Catharino, S. Walter, P. Feulner, A. Kromka, D. Steinmuller, and M. Stutzmann, "Protein-modified nanocrystalline diamond thin films for biosensor applications," *Nat. Mater.*, vol. 3, no. 10, pp. 736–742, 2004.

[17] V. Chakrapani, J. C. Angus, A. B. Anderson, S. D. Wolter, B. R. Stoner, and G. U. Sumanasekera, "Charge Transfer Equilibria Between Diamond and an Aqueous Oxygen Electrochemical Redox Couple," *Science*, vol. 318, no. 5855, pp. 1424–1430, Nov. 2007.

[18] H. A. Girard, J. C. C. Arnault, S. Perruchas, S. Saada, T. Gacoin, J.-P. Boilot, and P. Bergonzo, "Hydrogenation of nanodiamonds using MPCVD: A new route toward organic functionalization," *Diamond Relat. Mater.*, vol. 19, no. 7–9, pp. 1117–1123, Jul. 2010.

[19] J.-C. Arnault, T. Petit, H. Girard, A. Chavanne, C. Gesset, M. Sennour, and M. Chaigneau, "Surface chemical modifications and surface reactivity of nanodiamonds hydrogenated by CVD plasma," Physical Chemistry Chemical Physics, vol. 13, no. 24, pp. 11481–11487, 2011.

[20] H. A. Girard, T. Petit, S. Perruchas, T. Gacoin, C. Gesset, J. C. Arnault, and P. Bergonzo, "Surface properties of hydrogenated nanodiamonds: a chemical investigation.," Physical chemistry chemical physics : PCCP, vol. 13, no. 24, pp. 11517–11523, May 2011.

[21] T. Petit, H. A. Girard, A. Trouve, I. Batonneau-Gener, P. Bergonzo and J. C. Arnault, "Surface transfer doping can mediate both colloidal stability and self-assembly of nanodiamonds" (under review)

[22] J. A. Sergent, V. Paget and S. Chevillard, "Toxicity and Genotoxicity of Nano-SiO2 on Human Epithelial Intestinal HT-29 Cell Line". Ann Occup Hyg 2012, vol. 56, no. 5, pp 622-630, Jul. 2012.